


## Article

# POL-MUX System for Noncoherent Optical Networks

Radim Sifta <sup>\*,†</sup>, Michal Latal <sup>†</sup> , Petr Munster <sup>†</sup>  and Tomas Horvath <sup>†</sup> 

Department of Telecommunication, Brno University of Technology, Technicka 12, 616 00 Brno, Czech Republic; xlatal08@vutbr.cz (M.L.); munster@feec.vutbr.cz (P.M.); horvath@feec.vutbr.cz (T.H.)

\* Correspondence: radim.sifta@gmail.com; Tel.: +420-736-625-794

† These authors contributed equally to this work.

**Abstract:** This paper is focused on applying a polarization multiplex to passive optical networks to double their transmission bandwidth without significant changes in the distribution network. Although polarization multiplexes are already employed for high-speed optical transport networks with digital signal processing and coherent detection, we propose a system that could be used in existing older optical networks using a dynamic polarization controller in combination with a wavelength division multiplex.

**Keywords:** WDM; polarization; PDM; POL-MUX; PON; crosstalk; BER; DPC

## 1. Introduction

The demand for wider bandwidth in transport optical networks, as well as in optical access networks, increases every year. For this purpose, many multiplexing techniques have been developed, and some of them have been deployed for real data traffic. The most important multiplexing techniques in transport optical networks are the dense wavelength division multiplex (DWDM) and time division multiplex (TDM) [1]. The second generation of passive optical networks (PONs) uses both WDMs and TDMs [2]. Optical transport networks combine a DWDM with a polarization division multiplex (PDM) and coherent detection, thereby doubling the bandwidth. Although these systems are effective, it is not possible to use them for PONs due to digital coherent detection (DCD), which is the most expensive part. Nevertheless, there is a way to use a polarization multiplex without coherent detection.

Other multiplexing technologies have prospects for future deployment, but many of them are difficult to enforce because of the difficulty of implementation and necessity of intervention for the active components and distribution networks. This does not apply for polarization multiplexes, which can double the bandwidth without any intervention regarding the existing optical network, and in addition, such a multiplex is partially immune to polarization mode dispersion (PMD) [3]. The polarization multiplex (POL-MUX) is based on the transmission of two different optical signals in one optical fiber using polarization division. The optical beam in a single-mode fiber spreads in two polarization planes  $x$  and  $y$  that are orthogonal to each other. With a polarization beam splitter (PBS), it is possible to align independent optical signals into both polarization planes and transmit two different polarization-divided optical signals in one fiber.

The principle of polarization multiplexes can be compared with technologies used in radio systems, where radio signals are also transmitted in two orthogonal polarization planes and for receivers, two differently oriented antennas are used. Detection is possible only if the orthogonality of both signals is preserved. This is not possible in real optical fibers due to fiber imperfections (circular asymmetry of the fiber) and birefringence [4]. The basic scheme of the POL-MUX is shown in Figure 1.

An important advantage of the POL-MUX is that the distribution network does not need to be changed by any special component, as is this case for other multiplexing



**Citation:** Sifta, R.; Latal, M.; Munster, P.; Horvath, T. POL-MUX System for Noncoherent Optical Networks. *Appl. Sci.* **2021**, *11*, 5582. <https://doi.org/10.3390/app11125582>

Academic Editor: Amalia Miliou

Received: 15 May 2021

Accepted: 13 June 2021

Published: 16 June 2021

**Publisher's Note:** MDPI stays neutral with regard to jurisdictional claims in published maps and institutional affiliations.



**Copyright:** © 2021 by the authors. Licensee MDPI, Basel, Switzerland. This article is an open access article distributed under the terms and conditions of the Creative Commons Attribution (CC BY) license (<https://creativecommons.org/licenses/by/4.0/>).

techniques. On the transmitter side, two optical signals are aligned into a fiber by a polarization beam splitter (PBS), which has two inputs with polarization filters. The first input aligns the signal into the  $x$  plane, and the second input aligns the signal into the  $y$  polarization plane. Therefore, it is necessary to adjust the polarization angle so that each signal is parallel to the polarization axis of a given port. The polarization angle and state of polarization are set by a polarization controller (PC) [5].

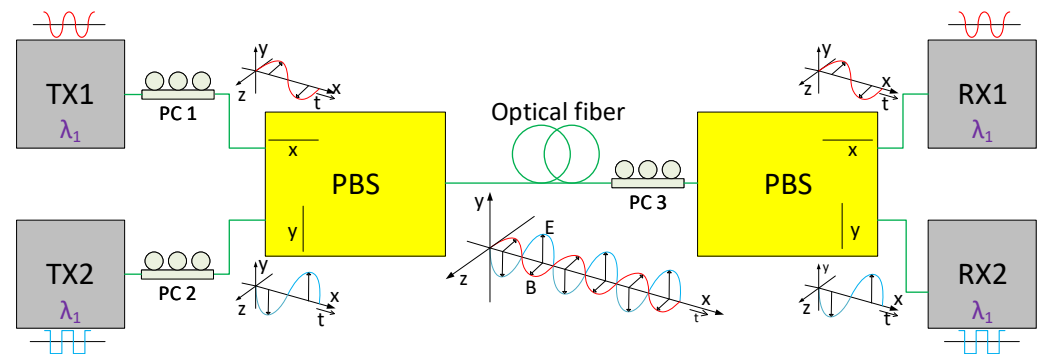


**Figure 1.** Principle of the polarization multiplex.

Multiplexed signals contain two differently modulated optical signals, which may have the same wavelength. These signals pass through an optical distribution network, at the end of which another polarization controller is used for rotation of the polarization process—each signal must be parallel to the polarization planes of the second polarization beam splitter, which is used for polarization demultiplexing. This ensures that the desired output signal is included in each polarization output [6].

Increasing the bitrate in optical networks tightens the requirements for polarization mode dispersion (PMD), which is the main limit of high-speed optical systems. Because a POL-MUX uses two separate polarization planes, a POL-MUX is not as influenced by PMD, as opposed to common telecommunication systems. This is very important for bitrates  $\geq 10$  Gbps. A POL-MUX can thus be used not only for doubling the bandwidth but also for reducing the influence of PMD, which has a negative effect in the form of polarization crosstalk [7].

POL-MUX system was the subject of research mostly in the 1990s and plenty of research groups were interested in this topic. Although it allows doubling of bandwidth and brings many advantages in comparison with other known multiplexing techniques, due to difficult demultiplexing, it was no longer prospective for further development, and WDM systems played the main role in the field of optical networks for many years [8–13]. The renaissance came after 2000, when the group of Yao et al. [5,6] engaged in research of POL-MUX systems using an all-optic scheme for polarization demultiplexing. Nevertheless, it was not employed in optical data networks and real a comeback occurred with the development of coherent high-speed networks with direct detection system, digital signal processing and multistate modulation formats. Many groups were interested in this topic [14–18], e.g., Bermiani et al. studied synchronous demodulation of coherent 16-QAM with feedforward carrier recovery [19], El-Nahal et al. described coherent 16 quadrature amplitude modulation (16QAM) Optical Communication Systems [20], Gnauck et al. examined spectrally-efficient long-haul WDM transmission using 224-Gb/s polarization-multiplexed 16-QAM [21]. Finally, direct detection systems with digital signal processing and X-QAM modulations were deployed into real high-speed transport optical networks, with high tolerance to negative dispersions effects [22].

On the other hand, there is also a disadvantage: difficult demultiplexing caused by changing the polarization angle and state of polarization. The principle of the POL-MUX system, shown in Figure 1 works only in laboratory environments. Under real conditions, the system must react to real-time polarization changes, such as those regarding the angle of polarization. For this purpose, a dynamic polarization controller could be used. In

coherent high-speed networks, a direct detection system is used, and demultiplexing is performed directly in the receiver via digital signal processing (DSP). Currently, 100 G transmission systems use POL-MUXs with coherent detection and multistate modulation formats [23]. The important parameters of the polarization multiplex are as follows [24]:

- Degree of polarization (DOP): The degree of polarization is given by:

$$DOP = I_{pol} / (I_{pol} + I_{unp}) \quad [-], \quad (1)$$

where  $I_{pol}$  and  $I_{unp}$  are intensities of polarized and nonpolarized light, respectively. If  $DOP = 0$ , we can say that the light is nonpolarized; if  $DOP = 1$ , the light is fully polarized. If the light is between 0–1, it is partially polarized.

- Polarization extinction (PER): The polarization extinction ratio is an important parameter given by the ratio between the optical powers in both polarization planes. It is defined by the ratio of the power in the principal polarization mode to the power in the orthogonal polarization mode after propagation through an optical system, expressed in dB [24].

$$PER = 10 \log_{10} \frac{P_{principal}}{P_{orthogonal}}. \quad [dB], \quad (2)$$

- Polarization dependent loss (PDL): The polarization-dependent loss is a parameter that specifies the maximal change in attenuation caused by polarization changes in optical fibers; this parameter is given also in dB.

## 2. Temperature Influence on the POL-MUX Signal

The angle and state of polarization are changed by mechanical stress and/or temperature. If the POL-MUX is deployed on an existing optical network, where the optical cables are fixed, then the temperature mainly rotates with the polarization angle, which is critical for the PER. For this reason, we measured the temperature influence on the change in the polarization angle of the optical network. To change the temperature of the testbed, a Vötsch VC3 7018 thermo chamber was used. The aim of the experiment was to determine the influence of temperature on birefringence and the change in the angle of polarization planes, e.g., how the power aligned with each polarization plane changes due to the rotation of polarization.

### 2.1. Principle of Measurement

The measurement testbed is shown in Figure 2. As a tested sample, a 10 m long optical patch cord with G.652.D fiber was used. The ambient temperature was kept at  $20 \pm 1^\circ\text{C}$ .

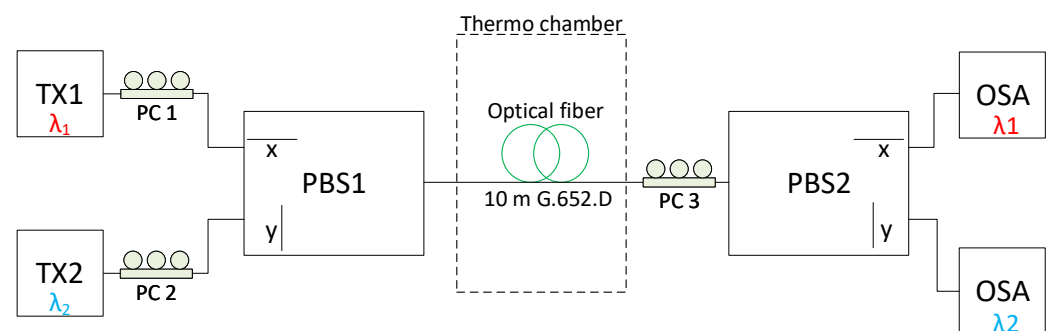


**Figure 2.** Block scheme of the measurement test bed.

As a light source, two laser diodes with different wavelengths ( $\lambda_1 = 1550.1$  nm and  $\lambda_2 = 1555.2$  nm) were used. Although it is possible to use the same wavelengths, we

used different wavelengths to enable the distinction of optical signals aligned with both polarization planes by a standard optical spectral analyzer (OSA). The optical signals from lasers TX1 and TX2 were set by polarization controllers PC1 and PC2, respectively, for optimal multiplexing by polarization beam splitter PBS1, e.g., the signal from one laser must be parallel to one of the polarization plane axes  $x$ , and the signal from the second laser must be parallel with polarization plane  $y$  of polarization beam splitter PBS1. The multiplexed signal is shown in Figure 3a. The optical powers of both lasers were set to  $TX1 = 5.61$  dBm and  $TX2 = 5.65$  dBm.

A multiplexed signal was fed into the testing optical patch cord, which was placed in a thermo chamber. The output of the tested fiber was connected to polarization controller PC3 and then to polarization beam splitter PBS2. Both outputs were checked by an optical spectral analyzer (OSA). The optimal setup of the state and especially the angle of polarization at the end of the measured optical link was carried out by PC3, so the polarization extension ratio was set to  $\geq 22$  dB according to the PBS datasheet. The demultiplexed signal is shown in Figure 3b. The default difference between the optical powers in each polarization plane was set to 23.22 dBm (measured by OSA $\lambda$ 1). We can say that it is optional to determine the noise ratio or crosstalk between polarization planes, which is given by the PER of PBS2.

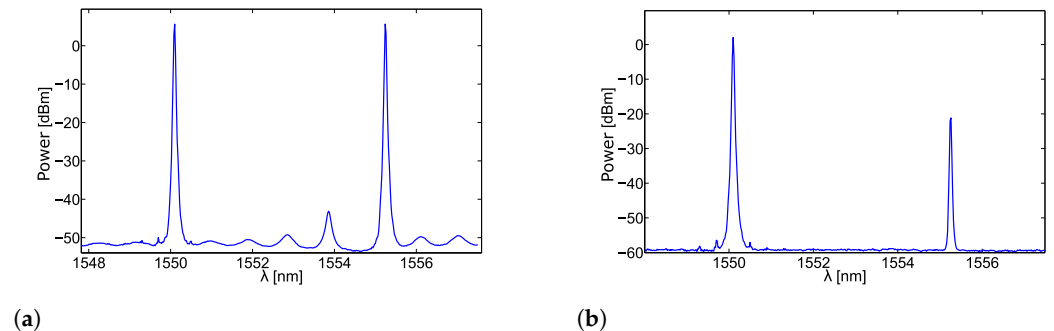


**Figure 3.** Spectra of the multiplexed (a) and demultiplexed (b) signals.

## 2.2. Experimental Analysis

The measurement process was divided into two parts. First, the measured fiber was cooled from  $20$  °C to  $-40$  °C and subsequently warmed back to  $20$  °C. Second, the fiber was warmed from  $20$  °C to  $70$  °C and cooled back to  $20$  °C. The 3D model in Figure 4 shows how the temperature changed the power in both polarization planes. A wavelength of  $1550.1$  nm corresponds to the output of the polarization splitter, which was monitored by the OSA. We mark this polarization plane as  $x$ .

During the cooling process, the temperature in the second polarization plane ( $y$ ) gradually increased up to  $-40$  °C when the power level increased from the original value  $-21.17$  dBm to  $0.74$  dBm. With further temperature increases, the power level decreased, and for  $20$  °C,  $-15.33$  dBm was achieved. After 30 min of tempering, the power level decreased to  $-24$  dBm. At the same time, it can be seen that in the polarization plane  $x$ , the power level was minimally decreased by approximately tenths of 1 dB. However, from  $-20$  °C to  $-40$  °C, it is possible to see a decrease in the power level with the highest minimum value ( $-4.15$  dBm) at  $-40$  °C, which is adequate as the maximal power level in-plane  $y$ . At this time, the angle of polarization was rotated almost  $90$  ° due to the changing ambient temperature. After further warming, the power level returned to the original level.

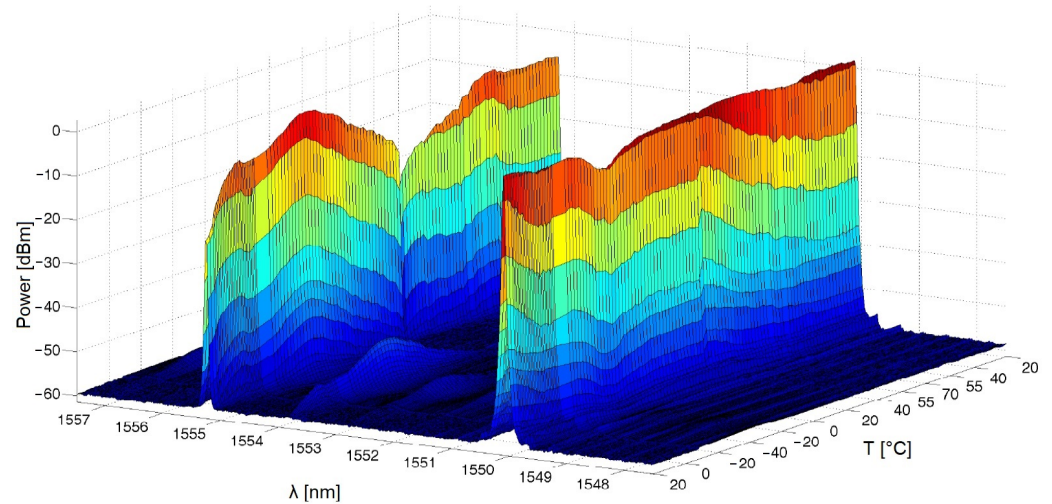


**Figure 4.** Power dependence on temperature in both polarization planes.

In the second part of the measurement, the fiber was warmed to  $+70^{\circ}\text{C}$ . The power level in the polarization plane  $y$  significantly increased as the temperature increased, with a maximum of  $-4.31$  dBm at  $70^{\circ}\text{C}$ . After that, the fiber was cooled to  $20^{\circ}\text{C}$ , and the power level decreased gradually to  $-21$  dBm. In polarization plane  $x$ , the power level decreased very slightly. Regarding the maximal power in plane  $y$  the power level in  $y$  decreased by only approximately 1 dB.

Figure 5 shows a comparison between the influences of cooling and warming on the change in the signal ratio between the polarization planes (in Figure 5, this is marked as the OSNR). It is obvious that the polarization angle is much more sensitive to temperatures below  $0^{\circ}\text{C}$  than to higher temperatures. The polarization planes were rotated almost  $90^{\circ}$  during the cooling process because the warming signal ratio between both signals was decreased; nevertheless, the polarization planes did not rotate like they did during cooling. Based on the analysis, we can say that if the temperature of the optical distribution network is kept within  $10^{\circ}\text{C}$ , the functionality of the POL-MUX system will be preserved even without the use of dynamic polarization control or DSP. A temperature change of  $10^{\circ}\text{C}$  caused the signal ratio between the polarization planes to be lower than 5 dB. Practical measurement confirmed that this value does not cause bit error rate (BER) degradation [25].

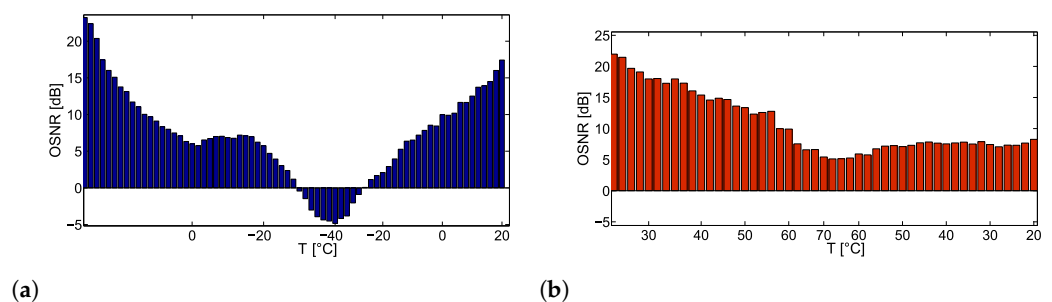


**Figure 5.** Influences of fiber (a) cooling and (b) warming.

### 3. POL-MUX on a Real Optical Network

After successfully demonstrating the POL-MUX in a laboratory environment, a bidirectional POL-MUX setup was tested on an optical network based on real academic data. In this case, the POL-MUX was used for the separation of 10 Gbps of downstream and upstream data traffic. The optical link consisted of a 12.8 km optical fiber between Brno University of Technology (BUT) and Masaryk University (MU), as shown in Figure 6. The

optical link was formed by five segments between six academy buildings and goes through a city with almost 400,000 residents and dense traffic. In the laboratory of transmission media, the Department of Telecommunication at BUT was placed on the first transmission and receiver side. As a transmitter, the EXFO FTB-1 platform with an EXFO NetBlazer 880G module and a 10G SFP+ module (Optoway SPS-2385MW-D440G) was used. The 880G module can generate high-speed 10 Gbps data traffic and measure the BER and quality of services (QoS) parameters. The wavelength was tuned to a 50 GHz DWDM grid with 1542.14 nm.

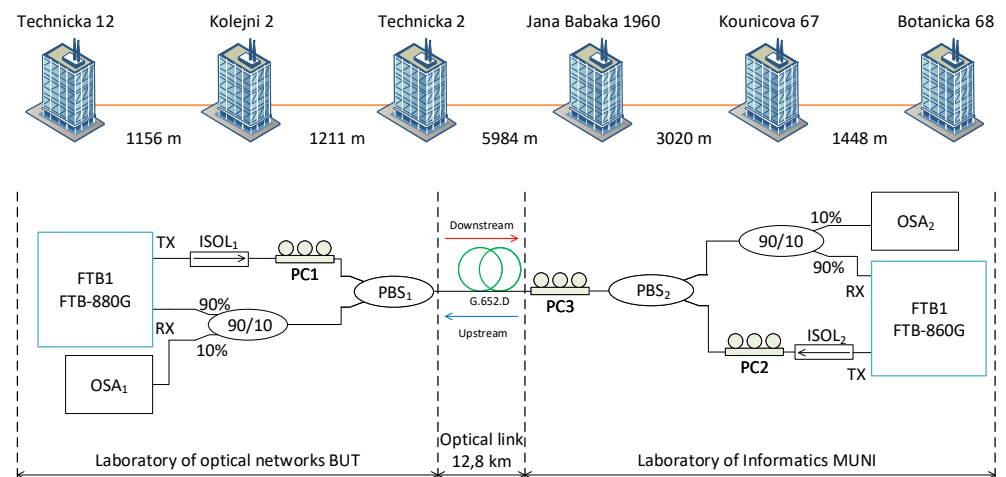


**Figure 6.** Measurement on a real optical link

The output signal from the SFP+ module went through an optical insulator  $ISOL_1$  (to avoid damage caused by back reflection) to a polarization controller  $PBS_1$ , where the angle of polarization was optimally rotated so that the optical signal of the output of  $PBS_1$  was at the maximum level (as measured by the OSA), which was then disconnected, and  $PBS_1$  was connected to a real optical link. The opposite transmission and receiver side was realized by the Faculty of Informatics at Masaryk University, Brno. The output signal from the optical link was controlled by  $PC_3$  to obtain the maximum power level of the output signal. This signal was monitored by an optical spectrum analyzer  $OSA_2$ .

As a transmitter on the opposite side, an EXFO FTB-1 platform with an EXFO NetBlazer 860G module and a 10 Gbps SFP+ module (Optoway SPS-2385MW-D440G) was also used. The 860G module has similar functionalities to those of 880G. The transmitted 10 Gbps signal went through  $ISOL_2$  to polarization controller  $PC_2$ , which was used to set the maximum optical level of an output of  $PBS_2$  (monitored by the OSA). The optical links consisted of many connector connections in each building. It is obvious that optical links are very prone to changes in polarization due to temperature changes.

The proposed POL-MUX network was measured for the bit error rate, which is one of the most important parameters with respect to QoS. The reason for this measurement was to determine how the time, temperature and possible mechanical stress changed the state and angle of polarization, which had a major impact on the power level in both polarization planes and of course on the bit error rate. Because the proposed system did not contain a dynamic polarization controller, we can say that the system was ‘static’ and was not able to react to changes in ambient conditions. The BER was tested for five days, and at the beginning of the test, the value of the BER was not measurable (too low) ( $>10^{-12}$ ). In the following days, the values were:

- 1st day–BER  $\approx 0$
- 2nd day–BER  $\approx 10^{-12}$
- 3rd day–BER  $\approx 10^{-11}$
- 4th day–BER  $\approx 10^{-10}$
- 5th day–BER  $\approx 10^{-8}$

Time changes of BER and data throughput are shown on Figure 7. As we can see, BER change in time was almost linear, very slowly reduced about one order per day. BER was in five days measurement reduced from 0 to  $\approx 10^{-8}$ . Data throughput is more resistant to polarization changes and was slightly reduced from 10 Gbps to 9.816 Gbps in five days. Table 1 also shows the change of power level measured by the optical spectral analyzer (10% of optical signal). As we can see, signal strength was reduced by about 9 dBm in five days. This practical measurement confirmed that polarization changes in the real optical network are slow and thus dynamic polarization controllers could keep the polarization angle of the transmitted signal.

**Table 1.** BER and throughput changes in time.

Time [Hours]	RX [dBm]	$\Delta$ [dBm]	BER [-]	T [Gbps]
0	-25.7	0	0	10
12	-28.7	3	0	10
24	-30.7	5	0	10
36	-31.2	5.5	$1.60 \times 10^{-12}$	10
48	-31.7	6	$9.50 \times 10^{-12}$	10
60	-32.2	6.5	$1.1 \times 10^{-11}$	10
72	-32.7	7	$3.10 \times 10^{-10}$	9.999
84	-33.2	7.5	$8.70 \times 10^{-10}$	9.997
96	-33.7	8	$1.40 \times 10^{-9}$	9.986
108	-34.2	8.5	$6.60 \times 10^{-9}$	9.94
120	-34.7	9	$1.90 \times 10^{-8}$	9.816

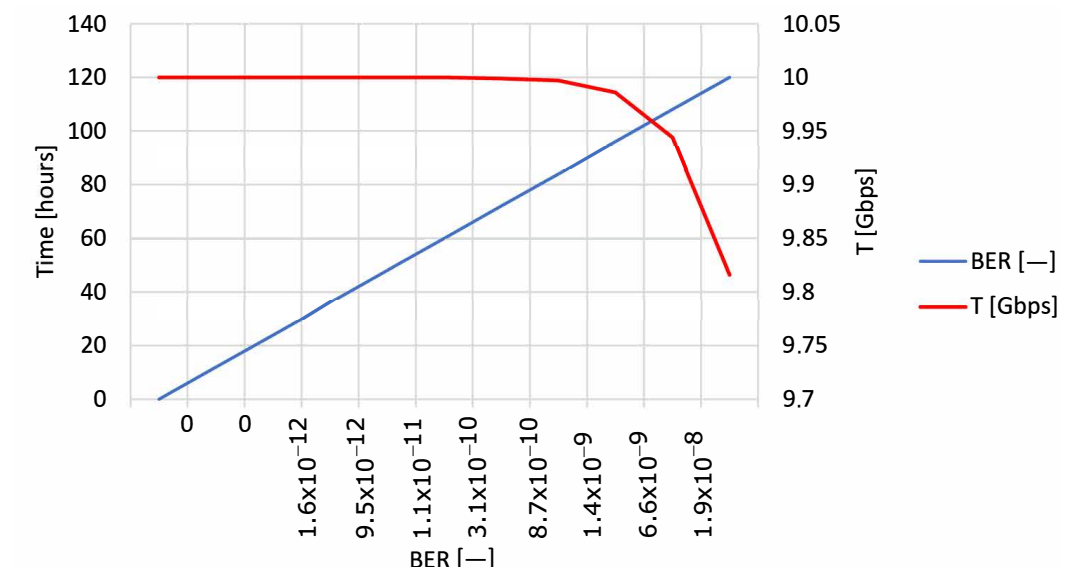


**Figure 7.** BER and data throughput on real optical network.

It is necessary to note that for both workplaces, the temperature was kept at a constant temperature by air conditioning, so the change in polarization was caused only by ambient conditions around the optical link between both workplaces. The measurement result is very important because although the system did not possess a dynamic polarization controller, there were no dynamic (fast) polarization changes. This means that if we employed a dynamic polarization controller, it should react to gradual temperature changes.

#### 4. Proposal of a Wide-Band Passive Optical Network (WDM-PDM-PON)

Based on knowledge gained from previous measurements, a simulation model of a wide-band passive optical network based on a polarization multiplex in combination with

a well-known wavelength division multiplex was designed. The system was designed in the VPItransmissionMaker(tm) Optical Systems simulation software [26].

#### 4.1. Theoretical Description

The POL-MUX system allows for the doubling of the transmission bandwidth, as mentioned before. However, the practical application of the POL-MUX is more effective in combination with other multiplexing systems. The polarization multiplex is transparent for other multiplexing technologies, so it can be easily used with a WDM, a TDM or other multiplexing technologies. Our model was designed as a combination of a PDM and a DWDM. This hybrid combination is called WDM-PDM-PON and allows the usage of  $n$  channels in the C or L band. Due to the polarization multiplex, it is possible to use the same wavelengths and thus double the bandwidth. The total bandwidth is given by the density of the wavelength multiplex and the number of possible DWDM channels according to the DWDM grid.

The principal polarization multiplex has been known for many years. The problem is utilizing effective demultiplexing to achieve an optimal ratio between the polarization planes and the corresponding crosstalk, which is harmed by polarization mode dispersion and polarization-dependent loss. Currently, 100 Gbps and 400 Gbps systems are demultiplexed by digital signal processing. This method has great demands for the use of state-of-the-art technologies and thus has high financial complexity. A dynamic polarization controller could be an effective way to maximize the fiber bandwidth with low-cost components.

The proposed WDM-PDM-PON is shown in Figure 8.  $n$ -channel multiplexed signals from wavelength multiplexers WDM-MUX1 and WDM-MUX2 are multiplexed by the polarization splitter PBS1. The multiplexed signals from both multiplexers carry different data at the same wavelengths. At the end of the optical link, using polarization demultiplexer PBS2, the two wavelength-multiplexed signals are split and fed to the corresponding demultiplexers WDM-DEMUX1 and WDM-DEMUX2. The advantage of this model is that a random number of wavelength channels could be multiplexed by one polarization multiplexer and demultiplexer; thus, only one dynamic polarization controller has to be used. On the other hand, the disadvantage of the proposed model is the necessity of utilizing polarization-maintaining (PM) fibers between all SFP transceivers and WDM multiplexers to maintain the polarization state and angle. The SFP transceivers are linearly polarized.

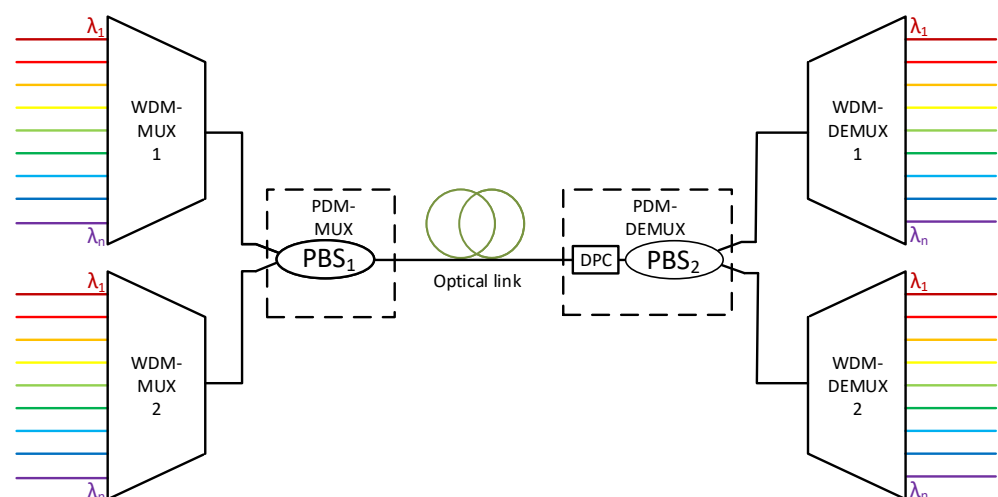


**Figure 8.** Block scheme of WDM-PDM-PON.

#### 4.2. Design of the Dynamic Polarization Controller–DPC

Due to the constantly changing angle of polarization in an optical transmission line, it is essential for the practical implementation of the POL-MUX to demultiplex signals in



a suitable way. As mentioned before, a dynamic polarization controller is able to quickly control changes in the polarization angle of the optical fiber and keep demultiplexed outputs automatically with minimal polarization crosstalk. Based on these requirements, a dynamic polarization controller was designed based on the patent in [3]. The block diagram of this controller is shown in Figure 9.

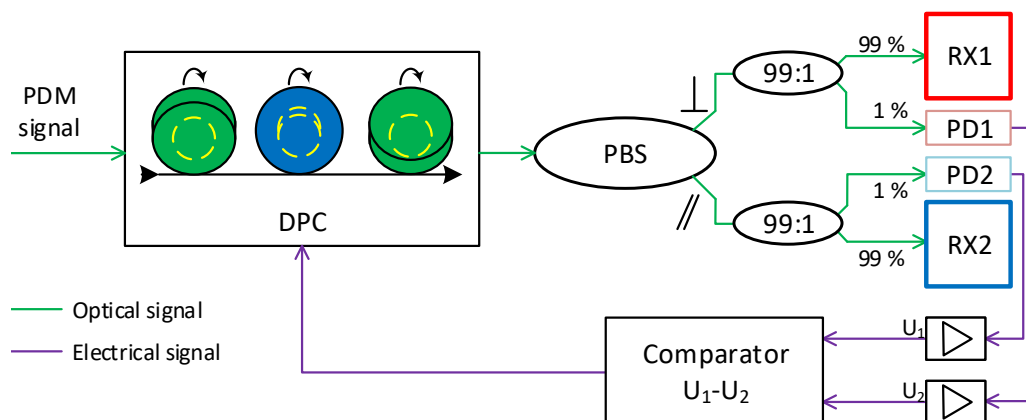


Figure 9. Block scheme of the dynamic polarization controller.

The input polarization multiplexed signal goes through the DPC to the PBS. The demultiplexed signal goes through the coupler with a division ratio of 99:1, where 99 % of the signal goes to receivers RX1 and RX2 and 1 % goes to monitoring photodiodes PD1 and PD2. The optical signal is converted to an electrical signal and amplified. The electronic comparator compares the voltage levels of both photodiodes PD1 and PD2 and regulates the DPC via servo-engines that rotate polarization by wave plates. The control signal from the comparator provides feedback that maintains the polarization in an ideal setup. The described system is independent of the bit rate and the modulated formats utilized. The next advantage is that the system does not need to interrupt the distribution network, transmitters, receivers and many other components used on optical links [3].

Optical signals with orthogonal polarization TX1 and TX2 could be generated by one laser diode or by two different diodes that transmit on the same wavelength. Both signals are multiplexed by a polarization multiplex. During the transmission of the multiplexed signal in the optical fiber, the state of polarization is changed from linear to elliptical. Importantly, both signals are orthogonal to each other. Let us choose polarization planes on the input of the polarization beam splitter as  $x$  and  $y$ . Mueller’s matrix of the polarization splitters is [6]:

$$M_x = \frac{1}{2} \begin{bmatrix} 1 & 1 & 0 & 0 \\ 1 & 1 & 0 & 0 \\ 0 & 0 & 0 & 0 \\ 0 & 0 & 0 & 0 \end{bmatrix}, \tag{3}$$

$$M_y = \frac{1}{2} \begin{bmatrix} 1 & -1 & 0 & 0 \\ -1 & 1 & 0 & 0 \\ 0 & 0 & 0 & 0 \\ 0 & 0 & 0 & 0 \end{bmatrix}. \tag{4}$$

An optical signal  $i$  with an arbitrary state of polarization (SOP) can be expressed in Stoke’s space as [6]:

$$\vec{S}_i = \begin{bmatrix} S_{i0} \\ S_{i1} \\ S_{i2} \\ S_{i3} \end{bmatrix} = \begin{bmatrix} P_i \\ P_i \cos 2\chi_i \cos 2\varphi_i \\ P_i \cos 2\chi_i \sin 2\varphi_i \\ P_i \sin 2\chi_i \end{bmatrix}, \tag{5}$$

where  $P_i$  is the optical power,  $\varphi_i$  is the angle of ellipticity (polarization) and  $\chi_i$  is the orientation angle of the  $i$ -th optical signal (see Figure 10). Behind the polarization beam splitter, the Stokes vectors along axes  $x$  and  $y$  are  $M_x \vec{S}_i$  and  $M_y \vec{S}_i$ , respectively. The first row of each Stoke's vector represents the optical power along the corresponding polarization plane [27]:

$$P_{ix} = \frac{1}{2}P_i(1 + \cos 2\chi_i \cos 2\varphi_i), \tag{6}$$

$$P_{iy} = \frac{1}{2}P_i(1 - \cos 2\chi_i \cos 2\varphi_i). \tag{7}$$

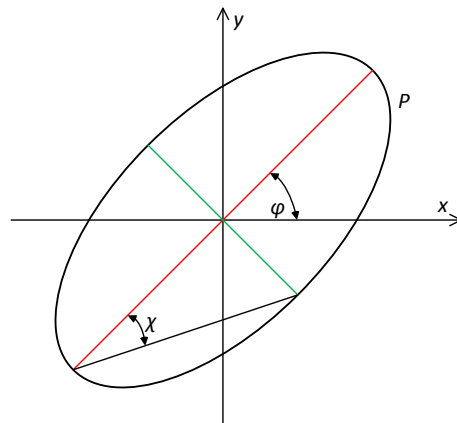


Figure 10. Polarization ellipse.

If both signals in the polarization planes are incoherent to each other (i.e., they are not generated from the same laser source), then the optical power of the corresponding polarization plane is:

$$P_x = P_{1x} + P_{2x} = \frac{1}{2}P_1(1 + \cos 2\chi_1 \cos 2\varphi_1) + \frac{1}{2}P_2(1 + \cos 2\chi_2 \cos 2\varphi_2), \tag{8}$$

$$P_y = P_{1y} + P_{2y} = \frac{1}{2}P_1(1 - \cos 2\chi_1 \cos 2\varphi_1) + \frac{1}{2}P_2(1 - \cos 2\chi_2 \cos 2\varphi_2). \tag{9}$$

For two optical signals with orthogonal states of polarization  $\vec{S}_1$  and  $\vec{S}_2$  [6]:

$$\chi_2 = -\chi_1, \tag{10}$$

where for angles  $\varphi_1$  and  $\varphi_2$ :

$$\varphi_2 = \varphi_1 + \frac{1}{2}\pi, \quad 0 \leq \varphi_1 \leq \frac{1}{2}\pi, \tag{11}$$

$$\varphi_2 = \varphi_1 - \frac{1}{2}\pi, \quad \frac{1}{2}\pi < \varphi_1 < \pi.$$

The substitution of Equations (6) and (7) into Equations (8) and (9) gives:

$$P_x = \frac{1}{2}(P_1 + P_2) + \frac{1}{2}(P_1 - P_2)\cos 2\chi_1 \cos 2\varphi_1, \tag{12}$$

$$P_y = \frac{1}{2}(P_1 + P_2) - \frac{1}{2}(P_1 - P_2)\cos 2\chi_1 \cos 2\varphi_1. \tag{13}$$

The optical powers from both polarization planes are monitored by photodetectors PD1 and PD2, which are realized by standard photodiodes. After conversion to an electrical signal, the corresponding difference of powers  $P_x - P_y$  in the optical area is given by the

difference between the photodiode voltages  $U_1 - U_2$  in the electrical area. This difference  $\Delta_U$  is the control and driving voltage of the DPC. The difference  $\Delta_U$  depends on the orientation angle  $\varphi$  and the angle of ellipticity  $\chi$ , which could be changed by the DPC. If  $\Delta_U = 0$ , then the crosstalk between both polarization planes is minimal and is given by the PER.  $\Delta_U = 0$  occurs at a positive maximum [3]:

$$\begin{aligned} \varphi = 0^\circ & \quad \chi = 0^\circ, \\ \varphi = \pm 90^\circ & \quad \chi = \pm 90^\circ, \end{aligned} \quad (14)$$

or at a negative maximum:

$$\begin{aligned} \varphi = \pm 90^\circ & \quad \chi = 0^\circ, \\ \varphi = 0^\circ & \quad \chi = \pm 90^\circ. \end{aligned} \quad (15)$$

#### 4.3. Simulation Model

The simulation model of WDM-PDM-PON is based on the idea described at the beginning of the paper—a combination of a DWDM and a POL-MUX used for multiplexing all WDM channels together. The block scheme is shown in Figure 11.

The central office (CO) is the main node that contains two OLT (optical line termination) units of the WDM-PON system. Each OLT contains 32 transmitters (TX1 to TX32) in the C-band (@1500 nm) with a 0.8 nm (100 GHz) DWDM grid. The pilot wavelength of the first transmitter is 1565.49 nm (191.5 THz), and that of the last transmitter (TX32) is 1540.56 nm (194.6 THz). The power level of the lasers was set to 1 mW (0 dBm) with the modulation format OOK-NRZ (on/off keying—no return to zero) and a bitrate of 10 Gbps. The data stream was generated by a pseudo-random bit sequence (PBRs) generator.

The output multiplexed signals from OLT1 and OLT2 were modified by polarization controllers PC1 and PC2 for optimal multiplexing by polarization splitter PBS1, e.g., the signal from one OLT must be parallel to one of the axes of polarization plane  $x$ , and the signal from the second OLT must be parallel with the polarization plane  $y$  of polarization beam splitter PBS2. The spectra of both output OLT signals are identical. The PER of the PBS was set to 25 dB.

Behind the CO is the first part of the optical distribution network ODN1, which consists of 10 km of G.652.D optical fiber. The parameters were set according to real fibers; the attenuation was 0.2 dB/km, the chromatic dispersion coefficient was 16 ps/(nm·km) and the coefficient of PMD was  $0.1 \frac{ps}{\sqrt{km}}$ . Before the fiber in ODN1 was placed, an attenuator with 3 dB of attenuation was placed to simulate the attenuation of the optical connectors.

Behind ODN1 is the first remote node (RN1) with polarization beam splitter PBS2 as a function of the polarization demultiplexer. The PER was set to 25 dB as for PBS1. The distribution network is further divided into two arms, ODN2 and ODN3, with the same fiber length of 5 km. The multiplexed WDM signals that carried 32 channels were demultiplexed in RN2 and RN3. The spectrum of the 17th demultiplexed channel is shown in Figure 12a, and the spectra of the other channels are shown in Figure 12b. The output demultiplexed signals were further fed via distribution networks ODN4–ODN68 to each optical network unit (ONU). The fiber length was set to 5 km, so the total length of the optical fibers was 20 km, which is standard for PON networks [28]. The ONU units consist of a photodetector and an OOK-NRZ demodulator. Effects of fiber attenuation, chromatic and polarization mode dispersion at 10 Gbps and 20 km long optical link do not influence transmitted signal, so we can focus on the polarization-related degradation.

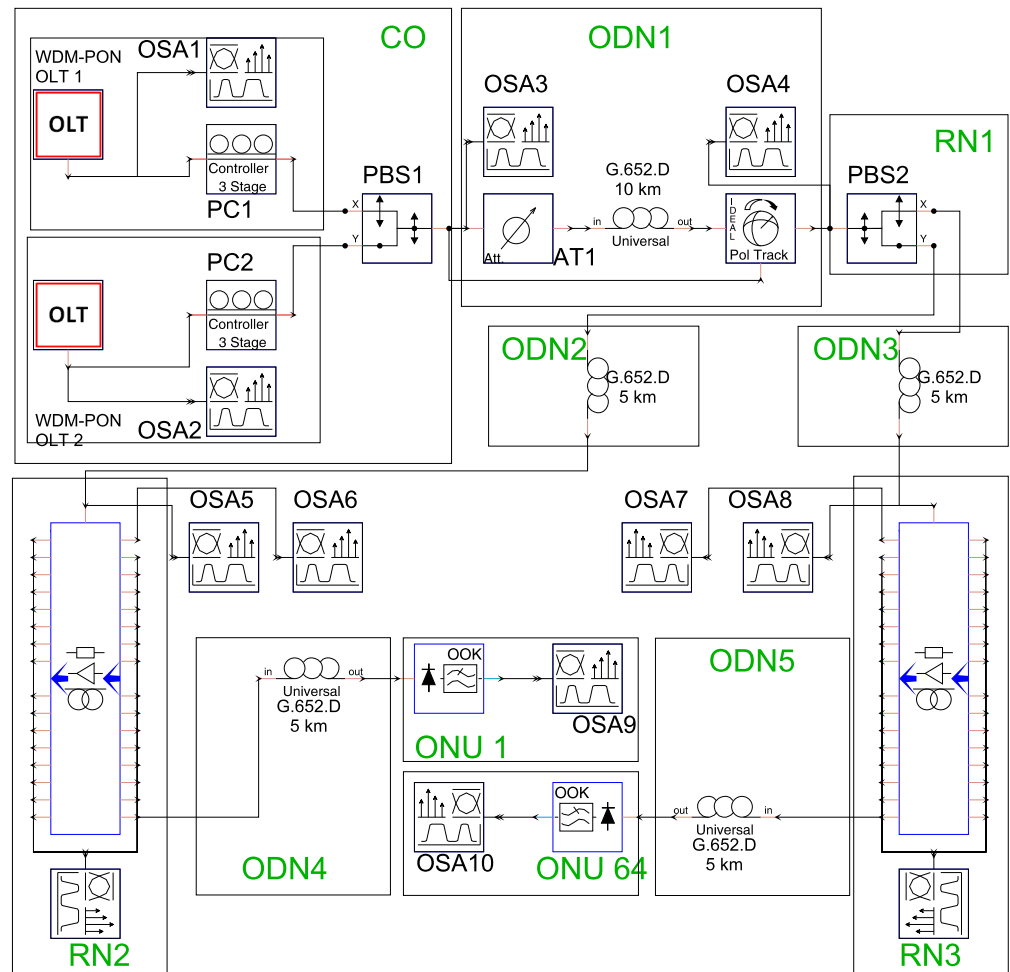


Figure 11. Simulation model of WDM-PDM-PON.

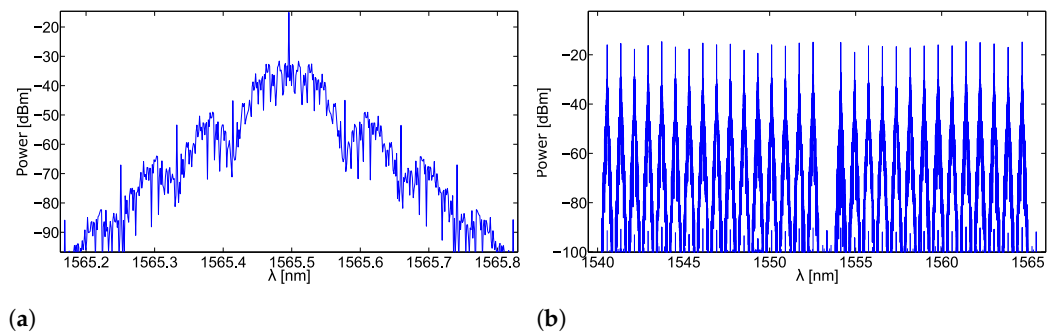
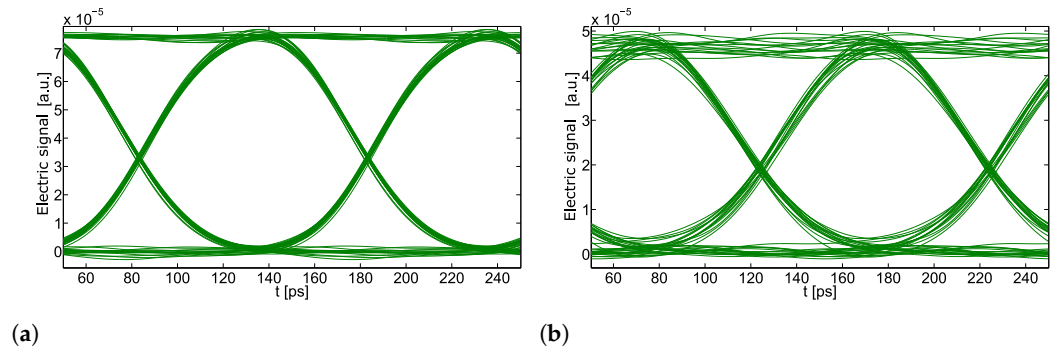


Figure 12. Spectra of other demultiplexed signals: (a) Spectrum of the 17th demultiplexed signal, (b) Spectra of other demultiplexed signals.

#### 4.4. Simulation Analysis

It is very important to observe how the changes in the PER values set for the polarization beam splitters affect the demultiplexed signal of each ONU unit. Assuming the usage of a dynamic polarization controller (block Pol. Track in the simulation model) the quality of the signal is dependent on the PER. The influence of this parameter can be compared by eye diagrams. Figure 13 shows how the eye diagrams change for PERs of 30 dB (a) and 15 dB (b). Figure 14 shows eye diagrams for PERs of 10 dB (a) and 5 dB (b).



**Figure 13.** Eye diagrams for different PER settings-(a) 30 dB, (b) 15 dB.

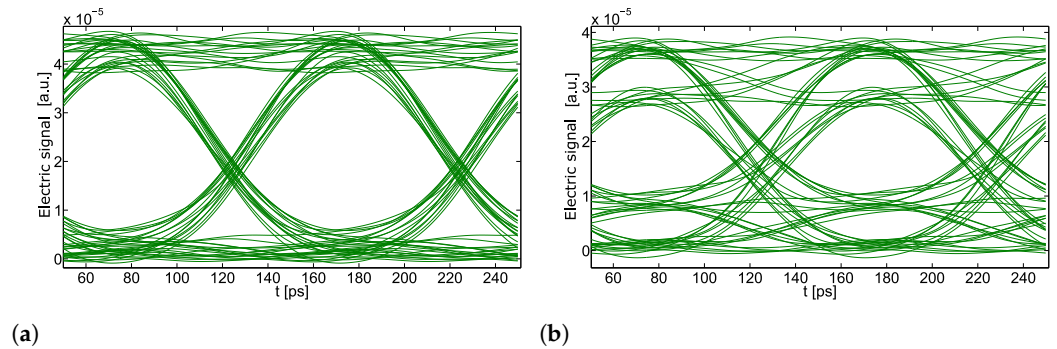


**Figure 14.** Eye diagram for different PER settings-(a) 10 dB, (b) 5 dB.

Eye diagrams show how decreasing the PER parameter gradually degrades the quality of the resulting signal.  $PER = 30$  dB is typical for high-quality polarization beam splitters, and as we can see in Figure 13, the output signal is not influenced (degraded) by the POL-MUX, and the eye diagram is clear, corresponding to a BER of  $10^{-25}$ . For the initial simulation,  $PER = 25$  dB, which is typical for commonly used polarization beam splitters. Additionally, for this setup, the signal quality is very good and corresponds to a BER of  $10^{-21}$ . With a further decrease in the PER, it is possible to see changes in the signal quality. For  $PER = 20$  dB, a BER of  $10^{-19}$  is observed and for  $PER = 15$  dB the BER is reduced to  $10^{-15}$ . Significant signal degradation occurs for  $PER = 10$  dB, as we can see from Figure 14, where the eye is closing and the BER is only  $10^{-11}$ . The most significant signal deterioration occurs when the PER is reduced to 5 dB, when the eye is significantly closed, and the bit error rate reaches only  $10^{-4}$ . The BER limit for PONs is  $10^{-12}$  [29].

Figure 15 shows Poincare spheres, where (a) corresponds to OSA1 and (b) corresponds to OSA2. The outputs from both OLT units contain the same WDM signals, both of which are linearly polarized. Before the PBS, both signals were set in terms of the polarization angle to match the polarization planes of the PBS, i.e., the signal from OLT2 was rotated approximately  $90^\circ$ . As is obvious from Figure 15, point S (Stokes parameter) is on the  $x$  and  $y$  planes and is on the surface of the sphere, which means that the signals are fully polarized ( $DOP = 1$ ).

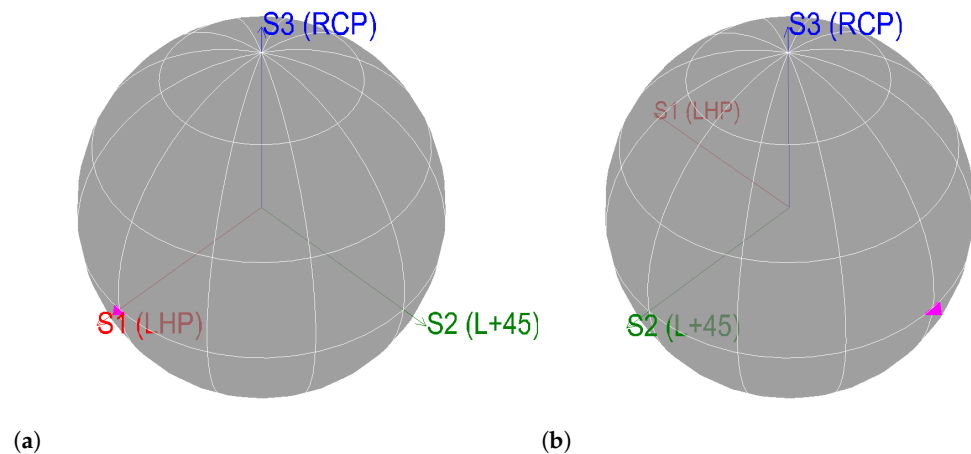


**Figure 15.** Poincare spheres of the multiplexed signals from OLT1 (a) and OLT2 (b).

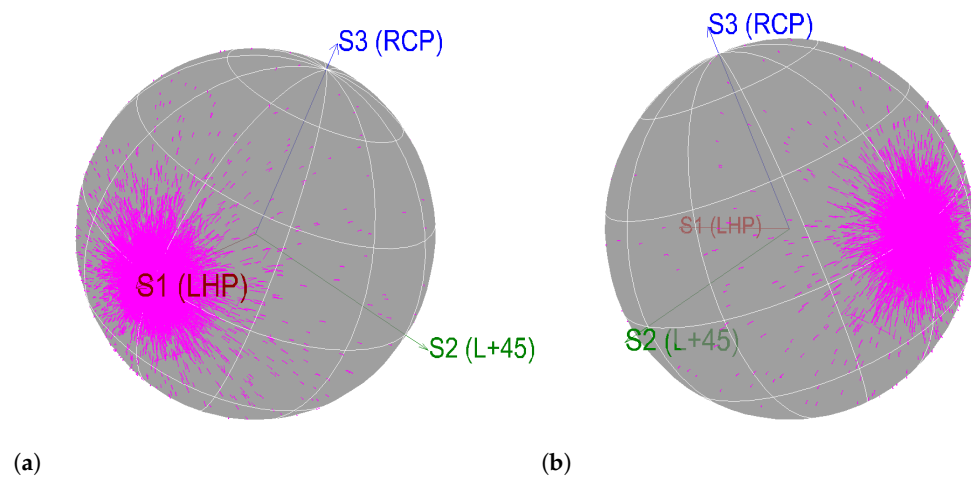


**Figure 16.** Poincare spheres of polarization demultiplexed signals from OLT1 (a) and OLT2 (b).

After the multiplexed signal passes through PBS1, the polarization partially changes from linear to elliptic, as shown in Figure 16. The use of a dynamic polarization controller can maintain the angle of polarization but not the state of polarization; nevertheless, this is not important for PON networks in which the detectors are insensitive to the state of polarization.

After the demultiplexed signal passes through the next 5 km of optical fibers (ODN2 and ODN3), the state of polarization is further changed based on theoretical assumptions from linear to elliptical, as shown in Figure 17a. Most of the points are concentrated in the  $x$  and  $y$  planes, so the signal is still partially linearly polarized. On the other hand, Figure 17b shows that signals in the second arm (ODN3) are concentrated along the  $z$  axis (S3), so we can say that it is partially circularly polarized (right-hand). The signals from both arms are fully polarized because all points are on the surfaces of the spheres.

Poincare spheres of the wavelength demultiplexed signals are shown in Figure 18. The spheres are formed by all points from all demultiplexed signals of the corresponding OLT units (different colors correspond to different wavelengths). As we can see, the spheres in Figures 17 and 18 are analogous, and the distributions of points are the same. Simulations confirm that polarization demultiplexing results in different states of polarization for different wavelengths but without any negative impact on signal quality.

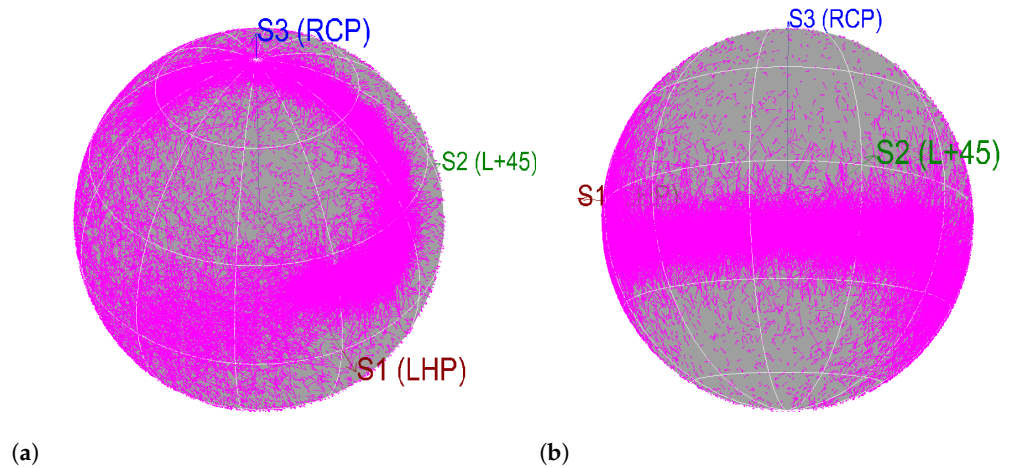


**Figure 17.** State of polarization before polarization demultiplexing ODN2 (a), ODN3 (b).

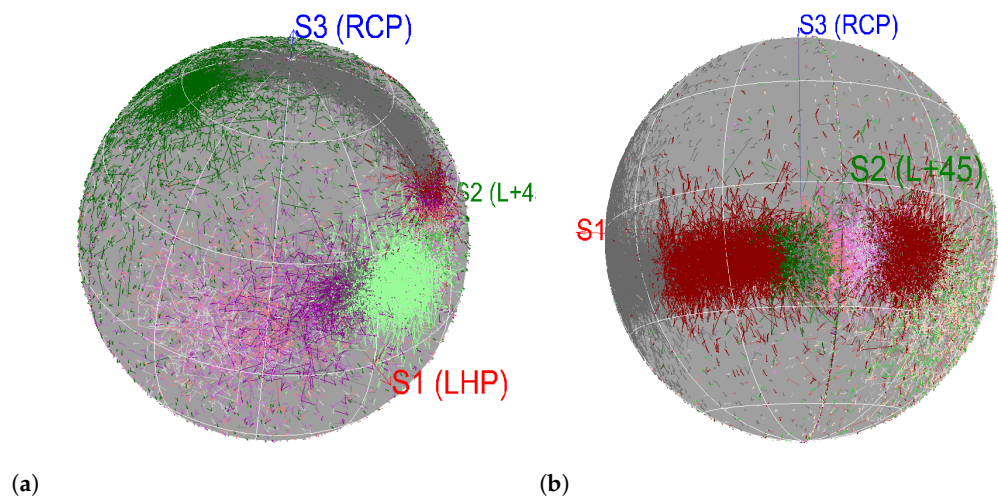


**Figure 18.** State of polarization after polarization demultiplexing OLT1 (a), OLT2 (b).

## 5. Conclusions

There are several ways to extend the bandwidths of optical networks, but many of these approaches are difficult to employ in existing distribution networks. Polarization multiplexes based on dynamic polarization controllers could be a possible method for passive optical networks where coherent detection with digital signal processing is not yet possible. Because mechanical stress and temperature are the factors that influence a POL-MUX system, the temperature dependence of the POL-MUX system was determined, and then a POL-MUX system based on a real academic optical network was tested. Based on the knowledge obtained from previous simulations and practical measurements, a simulation model of a wide-band passive optical network was proposed based on the idea of wavelength and polarization multiplexes. The proposed model demonstrated the functionality of this combination. Simulations verified the negative impact of reducing the PER on signal quality due to polarization crosstalk. Simulations and practical measurements also confirmed that changes in the polarization state do not influence the quality of optical signals for common PON networks. Future work will be focused on the development of DPCs and their implementations in real POL-MUX systems for PON networks.

**Author Contributions:** Conceptualization, R.S., P.M., T.H.; methodology, R.S., M.L., P.M., T.H.; validation, P.M., T.H.; formal analysis, R.S., M.L., P.M., T.H.; investigation, R.S., M.L., P.M., T.H.; resources, P.M., T.H.; data curation, R.S., M.L., P.M., T.H.; writing—original draft preparation, R.S., M.L., P.M., T.H.; visualization, R.S., T.H.; supervision, P.M.; project administration, T.H.; funding acquisition, T.H. All authors have read and agreed to the published version of the manuscript.

**Funding:** The research described in this paper was financed by a grant from the Ministry of the Interior of the Czech Republic, Program of Security Research, VI20192022135, for “Deep hardware detection of network traffic of next generation passive optical network in critical infrastructures”.

**Conflicts of Interest:** The authors declare no conflict of interest.

## References

1. Kaminov, I. *Optical Fiber Telecommunications (Sixth Edition)*; Academic Press: Berkeley, CA, USA, 2013. [[CrossRef](#)]
2. Prat, J. *Next-Generation FTTH Passive Optical Networks: Research Towards Unlimited Bandwidth Access*; Springer: Berlin/Heidelberg, Germany, 2008; ISBN 9781402084706.
3. Yao, X. Optical Communications Based on Optical Polarization Multiplexing and Demultiplexing. U.S. Patent 20050265728 A1, 27 May 2005.
4. Morant, M.; Pérez, J.; Llorente, R. Polarization Division Multiplexing of OFDM Radio-Over-Fiber Signals in Passive Optical Networks. *Adv. Opt. Technol.* **2014**. [[CrossRef](#)]
5. Yao, X.; Liu, L.; Wosinski, L.; He, S. Polarization beam splitter based on a two dimensional photonic crystal of pillar type. *Appl. Phys. Lett.* **2006**. [[CrossRef](#)]
6. Yao, X.S.; Yan, L.-S.; Zhang, B.; Willner, A.E.; Jiang, J. All-optic scheme for automatic polarization division demultiplexing. *Opt. Express* **2007**. [[CrossRef](#)] [[PubMed](#)]
7. Perlicki, K. A Simplified Analytical Model of Crosstalk in Polarization Division Multiplexing System. In Proceedings of the 5th Conference on Applied Electromagnetics, Wireless and Optical Communications, ELECTROSCIENCE'07, Tenerife, Spain, 14–16 December 2007; World Scientific and Engineering Academy and Society (WSEAS): Stevens Point, WI, USA, 2007; ISBN 978-960-6766-25-1.
8. Tsuji, R.; Hisano, D.; Takano, H.; Nakayama, Y.; Mishina, K.; Maruta, A. Remotely Pumped All-Optical Wavelength Conversion for WDM-PON-Based Access-Metro Convergence. *IEEE Photonics J.* **2021**, *13*, 1–10. [[CrossRef](#)]
9. Spolitits, S.; Murnieks, R.; Skladova, L.; Salgals, T.; Andrianov, A.V.; Marisova, M.P.; Leuchs, G.; Anashkina, E.A.; Bobrovs, V. IM/DD WDM-PON Communication System Based on Optical Frequency Comb Generated in Silica Whispering Gallery Mode Resonator. *IEEE Access* **2021**, *9*, 66335–66345. [[CrossRef](#)]
10. Kobayashi, T.; Shimizu, S.; Nakamura, M.; Umeki, T.; Kazama, T.; Kasahara, R.; Hamaoka, F.; Nagatani, M.; Yamazaki, H.; Nosaka, H.; et al. Wide-Band Inline-Amplified WDM Transmission Using PPLN-Based Optical Parametric Amplifier. *J. Light. Technol.* **2021**, *39*, 787–794. [[CrossRef](#)]
11. Yoshida, M.; Kan, T.; Kasai, K.; Hirooka, T.; Iwatsuki, K.; Nakazawa, M. 10 Channel WDM 80 Gbit/s/ch, 256 QAM Bi-Directional Coherent Transmission for a High Capacity Next-Generation Mobile Fronthaul. *J. Light. Technol.* **2021**, *39*, 1289–1295. [[CrossRef](#)]
12. Manso, C.; Muñoz, R.; Yoshikane, N.; Casellas, R.; Vilalta, R.; Martínez, R.; Tsuritani, T.; Morita, I. TAPI-enabled SDN control for partially disaggregated multi-domain (OLS) and multi-layer (WDM over SDM) optical networks [Invited]. *J. Opt. Commun. Netw.* **2021**, *13*, A21–A33. [[CrossRef](#)]
13. Ruggeri, E.; Tsakyridis, A.; Vagionas, C.; Kalfas, G.; Oldenbeuving, R.M.; van Dijk, P.W.L.; Roeloffzen, C.G.H.; Leiba, Y.; Pleros, N.; Miliou, A. A 5G Fiber Wireless 4Gb/s WDM Fronthaul for Flexible 360° Coverage in V-Band massive MIMO Small Cells. *J. Light. Technol.* **2021**, *39*, 1081–1088. [[CrossRef](#)]
14. Zhang, J.; Wu, W.; Ge, X. Time Reverse Equalization Algorithm for 16 QAM Coherent Optical Communication Systems. *IEEE Access* **2021**, *9*, 60753–60763. [[CrossRef](#)]
15. Catanese, C.; Ayassi, R.; Pincemin, E.; Jaouen, Y. A Fully Connected Neural Network Approach to Mitigate Fiber Nonlinear Effects in 200G DP-16-QAM Transmission System. In Proceedings of the 2020 22nd International Conference on Transparent Optical Networks (ICTON), Bari, Italy, 19–23 July 2020; IEEE: Bari, Italy, 2020; pp. 1–4.
16. Sharma, S.; Krishnamurthy, P.K. Laser and Nonlinear Phase Noise Tracking and Estimation in Long Haul 400 Gbps Single Carrier PDM-16-QAM Systems using Multi-step Kalman Filter. In Proceedings of the 2020 International Conference on Signal Processing and Communications (SPCOM), Bangalore, India, 19–24 July 2020; IEEE: Bangalore, India, 2020; pp. 1–4.
17. AL-QADI, M.; Laperle, C.; Charlton, D.; O’Sullivan, M.; Xie, C.; Hui, R. Multichannel 16-QAM Single-Sideband Transmission and Kramers—Kronig Detection Using a Single QD-MLL as the Light Source. *J. Light. Technol.* **2020**, *38*, 6163–6169. [[CrossRef](#)]
18. Kamran, R.; Naaz, S.; Goyal, S.; Gupta, S. High-Capacity Coherent DCIs Using Pol-Muxed Carrier and LO-Less Receiver. *J. Light. Technol.* **2020**, *38*, 3461–3468. [[CrossRef](#)]
19. Al-Bermani, A.; Wordehoff, C.; Hoffmann, S.; Pfau, T.; Ruckert, U.; Noé, R. Synchronous demodulation of coherent 16-QAM with feedforward carrier recovery. *IEICE Trans. Commun.* **2011**, *94*, 1794–1800. [[CrossRef](#)]
20. El-Nahal, F.I. Coherent 16 quadrature amplitude modulation (16QAM) Optical Communication Systems. *Photon. Lett. Pol.* **2018**, *10*, 57–59.



21. Gnauck, A.H.; Winzer, P.J.; Chandrasekhar, S.; Liu, X.; Zhu, B.; Peckham, D.W. Spectrally efficient longhaul WDM transmission using 224-Gb/s polarization-multiplexed 16-QAM. *J. Light. Technol.* **2011**, *29*, 373–377.
22. Badraoui, N.; Berceci, T. Enhancing capacity of optical links using polarization multiplexing. *Opt. Quantum Electron.* **2019**, *51*, 310. [[CrossRef](#)]
23. Oktem, T.; Erdogan, A.; Demir, A. Adaptive Receiver Structures for Fiber Communication Systems Employing Polarization-Division Multiplexing. *Light. Technol. J.* **2009**. [[CrossRef](#)]
24. Jeong, J. *Fiber Optic Polarization–Polarization Control and Measurement for Optical Fibers*; Newport: Irvine, California, USA, 2006.
25. Sifta, R. Quality of Services in Optical Access Networks. Dissertation Thesis, Brno University of Technology, Brno, Czech Republic, 2015.
26. VPIphotonics: Simulation Software and Design Services. Available online: <https://www.vpiphotonics.com/index.php> (accessed on 11 May 2021).
27. Nelson, L.; Nielsen, T.; Kogelnik, H. Observation of PMD-induced coherent crosstalk in polarization-multiplexed transmission. *IEEE Photonics Technol. Lett.* **2001**. [[CrossRef](#)]
28. Tanaka, K.; Agata, A.; Horiuchi, Y. IEEE 802.3av 10G-EPON Standardization and Its Research and Development Status. *J. Light. Technol.* **2010**, *28*, 651–661. [[CrossRef](#)]
29. Girard, A. *FTTx PON Technology and Testing*; EXFO: Quebec City, QC, Canada, 2005.